Effect of Electrodes on Electronic Transport of Molecular Electronic Devices†

Yeonchoo Cho, Woo Youn Kim,* and Kwang S. Kim*

Center for Superfunctional Materials, Department of Chemistry, Pohang University of Science and Technology, San 31, Hyojadong, Namgu, Pohang 790-784, Korea

Received: November 28, 2008; Revised Manuscript Received: February 26, 2009

Understanding the effects of each component of a molecular device is at the heart of designing a useful device. Molecular cores and linkers are well studied, but relatively few studies have been devoted to investigating the electrode effect on a molecular electronic device. Here, we study unique characteristics of Au, Ru, and carbon nanotube electrodes using the nonequilibrium Green function method combined with a density functional theory. By systematic modification of the device region, we extract the effect of the electrode materials on the electron transport. We show that the band structure and surface density of states of an electrode material, independent of the choice of other device components, have unique influences on the transmission curve. We note that carbon nanotube electrodes can offer unusual nonlinear current−voltage characteristics.

I. Introduction

Molecular electronics would be the most probable alternative to the silicon-based electronics slowly approaching to the limit of miniaturization.[1] Since Aviram and Ratner suggested the possibility of using a single molecule as a rectifier,[2] Reed et al. first measured the current−voltage ($I-V$) characteristics of the dithiol benzene system self-assembled to the Au electrodes,[3] and further advances have been achieved.[4,5] Theoretical approaches have also been exploited. Some of them are tight-binding models,[6,7] while others are based on density functional theory (DFT) calculations.[8−11] After these initiatives, the steps toward device design based on a single molecule have been made. Numerous researches have focused on finding new device molecules to substitute any conventional electric component as well as to act as a new type of Components exploiting quantum nature.[12−18]

For the design of a useful device, it is important to clarify what role each part plays in a molecular electronic device. Effects of a linker, which is a functional group connecting between a molecule and electrodes at both sides, have been intensively studied because the linker, being more than a simple glue, significantly modifies the electronic structure of a device molecule and thereby the transport properties.[5,19,20] In contrast to linkers, few studies have been devoted to the comparison of different electrodes. Most of them regarded an electrode just as a part of contact.[21−24] Namely, electrode effects are reduced to those of a few electrode atoms on contact, limiting the electrode effects to determining contact geometry and chemical bonding between individual atoms. However, we can obviously expect that as a linker is more than just a glue, an electrode should play a more profound role than a mere constituent of contact, as is evident from its semi-infinite nature.

In this study, we compare the effects of Au, Ru, and carbon nanotube (CNT) electrodes on molecular electronic devices. Au is the most popular electrode material in molecular electronics. Au electrodes can be readily connected to a device molecule by gold thiol self-assembly.[25] Tulevski et al. studied the Ru surface[26] to which a carbon atom was bound by forming a multiple covalent bond. Guo et al. studied CNT electrodes with an amide linkage.[27] CNTs have received considerable attention as electronic devices due to their one-dimensional characteristics, metallic properties, and so forth.[28−32] Here, we regard Au, CNT, and Ru as representative materials having s, p, and d band characters in the vicinity of their Fermi energies, respectively.

We study the three electrodes using DFT coupled with the nonequilibrium Green's function (NEGF) scheme.[33] This coupled method has reasonably reproduced experimental data.[34] To compare the effects between different electrode materials, we use a simple conductive molecule, 1,3,5-hexatriyne (which we will call "alkyne" for convenience's sake).[35] Transmission curves are calculated after attaching each type of electrodes to both ends of the molecule. Successive transmission calculations are made to extract influences solely from electrodes by modification of a molecular core and linkers. The band structure and surface density of states (SDOS) of each electrode material are compared to the transmission function of each system under a zero bias, and the consequences of the electrode material on molecular electronic devices are discussed.

II. Calculation Methods

We perform DFT calculations of a molecule in contact with semi-infinite electrodes. All of the calculations are carried out using POSTRANS,[33] in which the NEGF code is implemented in the DFT program of the Spanish Initiative for Electronic Simulations with Thousands of Atoms (SIESTA[36]). The implemented NEGF code is adequate to deal with large systems by efficient memory management and parallelization. The generalized gradient approximation by Perdew−Burke−Ernzerhof (PBE[37]) is used in all calculations. The standard single-ζ polarization basis set is primarily used, while the double-ζ basis set is used for Ru. A grid cutoff is 150 Ry.

† Part of the "George C. Schatz Festschrift".

* To whom correspondence should be addressed. E-mail: kim@postech.ac.kr (K.S.K.); rodman@postech.ac.kr (W.Y.K.).

10.1021/jp810467q CCC: $40.75
Published on Web 03/13/2009

We calculate steady-state currents by adopting the Landauer−Buttiker formula

$$I(E, V) = \frac{2e}{h}\int_{-\infty}^{\infty} T(E, V)[f(E - \mu_L) - f(E - \mu_R)]\mathrm{d}E \quad (1)$$

where $T(E,V)$ is the transmission probability as a function of energy E and bias voltage V, and f, μ, e, and h are Fermi−Dirac distribution function, chemical potential, electron charge, and Planck constant, respectively. The transmission function involves damping functions and Green functions as shown below:

$$T(E, V) = \mathrm{Tr}[\Gamma_L(E, V)G(E, V)\Gamma_R(E, V)G^{\dagger}(E, V)] \quad (2)$$

Here the damping function $\Gamma_{L/R}(E,V)$ and the Green function $G(E,V)$ are formulated as follows:

$$\Gamma_{L/R}(E, V) = \mathrm{i}[\Sigma_{L/R}(E, V) - \Sigma_{L/R}^{\dagger}(E, V)] \quad (3)$$

$$G(E, V) = [ES_M - H_M - \Sigma_L(E, V) - \Sigma_R(E, V)]^{-1} \quad (4)$$

where $\Sigma_{L/R}(E,V)$ is the self-energy as a function of energy (E) and bias voltage (V) and L/R is a label for the left/right lead and M represents the device molecule part.

The self-energy involves all of the contact effects on the molecule region due to the electrodes, so that it plays a critical role in determining the transport characteristics of a device. It is made up of the surface Green function $[g^s(E)]$ of the electrode and the term $[\tau(E)]$ representing interaction between the electrode and the molecular parts:

$$\Sigma_{L/R}(E, V) = \tau_{L/R}^{\dagger}(E, V)g_{L/R}^{s}(E, V)\tau_{L/R}(E, V) \quad (5)$$

The surface Green function $[g_{L/R}^{s}(E,V) = (ES_{L/R} - H_{L/R})^{-1}]$ is computed from the Hamiltonian ($H_{L/R}$) and overlap matrices ($S_{L/R}$) of a semi-infinite structure of the electrode using the transfer matrices method.[38] It is also used when calculating SDOS, that is, SDOS $= -\pi^{-1}$ Im[Tr(g^sS)]. This scheme enables an accurate description of electrodes. The details of the formalism are summarized elsewhere.[33]

The whole procedure, in practice, is optimization of the geometry and subsequent calculations of the transmission function. The scattering region of the system includes a few layers of the leads and a sandwiched device molecule. Figure 1 shows the optimized structures of the scattering region. In constructing these regions for the Au and Ru electrodes, the device molecule is placed above the center of a triangle in Au(111) and Ru(111) surfaces, respectively. For CNT, the molecule is connected to the metallic CNT(5,5) electrodes through a sulfur linkage. The geometry of a device molecule and the lead−lead distance are optimized while freezing the geometry of the electrodes. Using the optimized geometries, the transmissions are calculated under a finite or zero bias.

Since this study attempts to reveal the electrode effect, a realistic modeling of electrodes is of utmost importance. We believe that our method is currently the best possible approach to study the electrode effect. First, the electrode part is treated on an equal footing with the scattering region at the DFT level. Second, the surface Green function from which the self-energy matrix is computed is calculated from the realistic atomic crystal

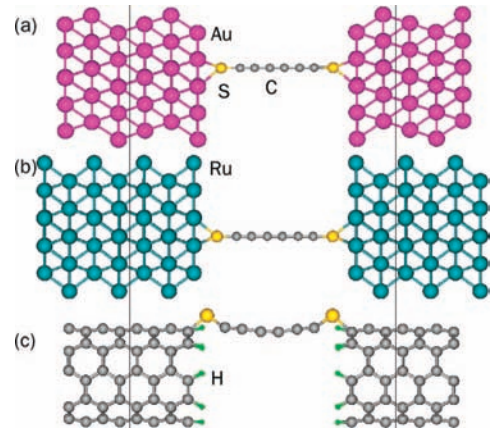

Figure 1. Selected optimized geometries of (a) the Au−S alkyne system, (b) the Ru−S alkyne system, and (c) the CNT−S alkyne system. Size scales are not identical to each other. Note that the scattering region (a central region separated from the electrode region by black lines) includes several layers of electrodes as well as a device molecule and contact regions. The remaining ones represent the periodic unit cells of electrode parts.

structure without resorting to the cluster approximation and the tight-binding approximation, which may add artifacts to calculation results. Finally, the sufficient number of k points is sampled to accurately take into account the semi-infinite, bulk nature of electrodes. In the calculations, we first increase the number of k points sampled along the surface normal directions until the transmission curve converges. This enables one to fully take into account the infinite surface effect of electrodes. In the Au case, the results with 5×5 k points were already converged, while in the Ru case, the 7×7 k point sampling was used.

Some well-known difficulties should be noted. Usually, theoretical conductance values are higher than experimental values when metal−molecule junctions are used. The applied theoretical approach tends to overestimate the current for the metal electrode systems due to the limitation of the used exchange-correlation functionals as well as the self-interaction error.[39−41] To include electron correlation effects properly, a GW approximation would be employed for simple systems.[42] However, for the complicated systems to compare different electrodes, the present approach would be the most useful in a practical point of view. Given that the bond length between the end atom of a molecule and an electrode is short, the systems studied here are near to the strong coupling limit. Thus, the influence of the self-interaction errors on conductance would be small.

III. Results and Discussion

The contact effects due to the electrodes are to renormalize the electronic structure of the device molecule. In eq 4, the Green's function can be rewritten by defining an effective Hamiltonian ($H_{eff} = H_M + \Sigma_L + \Sigma_R$) as follows:

$$G(E, V) = [ES_M - H_{eff}]^{-1}$$

The effective Hamiltonian presents the renormalized Hamiltonian of the device molecule. The semi-infinite nature of the electrodes is explicitly involved through self-energy terms whose real/imaginary parts give rise to a shift/broadening of the molecular energy levels. While the electrode parts provide the surface Green's function (g^s) in the self-energy term as shown in eq 5, the linker parts determine the interaction term (τ).

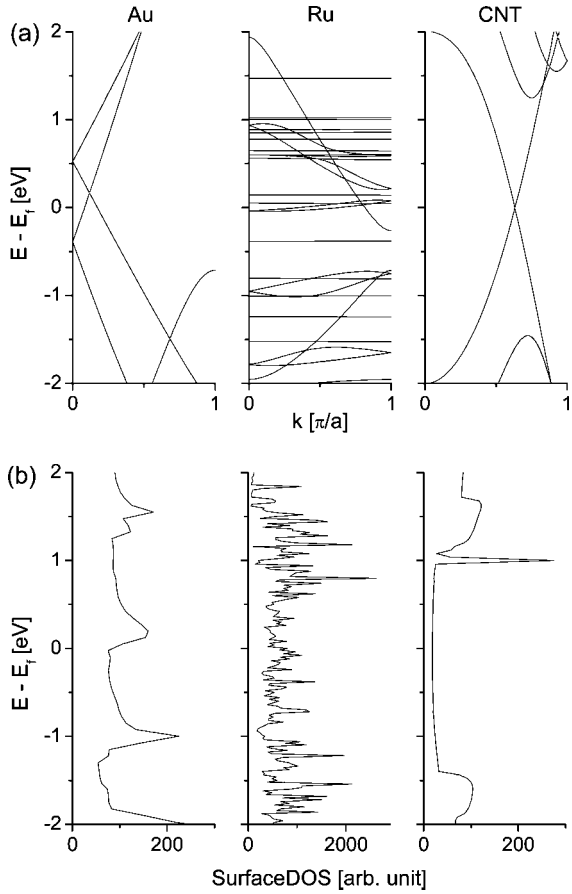

Figure 2. (a) Band structures of the Au, Ru, and CNT unit cells presented as electrode parts in Figure 1. The direction of k is parallel to the direction of electron flow. (b) Surface density of states (SDOS) of Au, Ru, and CNT. The "surface" means the interface between the semi-infinite electrodes and the scattering region including a few layers of electrodes at both ends (refer to Figure 1).

Alignment of molecular energy levels with respect to the Fermi energy of the leads is directly related to the transmission functions. Hence, the different SDOSs for the three different types of electrode materials should give different transmission functions.

To this end, we first discuss the properties of electrode materials relevant to the device's characteristics, (i) the band structures of electrode materials, which show the characteristics of electronic states involved in electron transport, and (ii) their SDOS, which gives the information of electron reservoirs related to how many states can accept or supply electrons that constitute current flow (Figure 2). Au has broad bands over a wide energy range. These must be 6s orbitals because the 6s state is the highest occupied molecular orbital (HOMO) for a Au atom. The SDOS curve of Au shows even distribution of states, except for small bumps almost at every 1 eV interval due to the surface effects, which is contrasted with the flat DOS of the bulk Au. Flat lines in the Ru band structure stem from the valence d orbitals. Although Ru has some broad bands around the Fermi energy, many flat d bands mainly contribute to the SDOS. In the case of CNTs, the p bands are the valence which solely contributes to the SDOS around the Fermi energy. Other bands begin to play when the energy is different from the Fermi energy by more than 1 eV. The SDOS of the metallic CNT(5,5) has relatively large and broad peaks above 1 eV and below −1 eV, whereas such peaks are absent between −1 and 1 eV. This is the unique feature of CNTs in contrast with the other metals.

We find that the position and broadening extent of peaks in the transmission curve with different electrodes have different aspects from one another, though the same device molecule and linkages are employed. Figure 3a shows transmission curves where Au, Ru, and CNT electrodes are connected to a linear alkyne molecule via sulfur linkages. In the case of Au, the HOMO peak covers the Fermi energy, and the lowest unoccupied molecular orbital (LUMO) peak is so distant from the Fermi energy that only the edge is seen in the figure. In contrast, the Fermi energy is equidistant from the HOMO and LUMO peaks in the cases of Ru and CNT. The large work function of Au might be relevant. Regarding the extent of broadening, the transmission curve of the Au-contacted system has conspicuous peaks, but these peaks are too broad to be completely separated. Because of the large peak around the Fermi energy corresponding to the HOMO of the alkyne, a comparably large current is expected even under a small bias. In the Ru case, broad peaks are observed, but they seem to be made up of many sharp peaks. The HOMO and LUMO peaks can be distinguished, though the exact positions are not well defined. Since metals have many states nearby the Fermi energy, it is probable to have appreciable transmission values through this range. On the other hand, when CNT electrodes are employed, discrete and narrow peaks appear, and transmission peaks are either nonexistent or diminutive in the region of small SDOS between the peaks, that is, between −1 to 1 eV.

Since the contact structure has a profound effect on the characteristics of a device, the features we discussed may have originated from the linkage and device molecule rather than the electrodes. Thus, we perform the same calculations without sulfur linkers in order to extract the electrode aspect from the contact effect (Figure 3b). Different peak positions and the HOMO−LUMO gap are expected because removing linkers essentially means that the sandwiched molecule is changed to a different one. Indeed, removal of linkers induces changes in positions of the HOMO and LUMO peaks relative to the Fermi energy. This fact needs special attention when one designs a device molecule because a linker is not only just a glue but also acts as a band-lineup modifier. Both metals preserve nonzero transmission at the Fermi energy. When comparing different electrodes, the tendency of broadening remains similar, as expected, corroborating our proposition that electrodes shape transmission peaks. Smooth/rugged shapes for Au/Ru electrodes are conserved as well. The Au-contacted system shows more broadening; HOMO and LUMO peaks are highly overlapped. In the Ru case, the transmission curve varies rapidly, and it is difficult to define molecular peaks corresponding to the HOMO or LUMO. In the case of a CNT, the HOMO peak becomes slightly smaller, and the LUMO peak grows up. Nonetheless, they are well distinguished from other peaks. Transmission values are still very low around the Fermi energy.

This trend remains even if a device molecule is changed. In Figure 3c, we present the transmission curves of a *p*-dithiol benzene molecule sandwiched by Au, Ru, and CNT electrodes. Before looking into the transmission curves, the difference between alkyne and benzene should be noted. The HOMO−LUMO gap of 1,3,5-hexatriyne is about 3.5 eV within DFT calculations, whereas that of benzene is 4.9 eV. When including sulfur linkers at both ends, the gap is reduced to 2.1 and 3.5 eV, respectively. Relative HOMO and LUMO positions in the transmission curves according to the type of electrodes do not change when a molecule is changed; the HOMO peak is much closer to the Fermi energy in Au than the LUMO peak, and both HOMO and LUMO peaks are almost equidistant from the Fermi energy

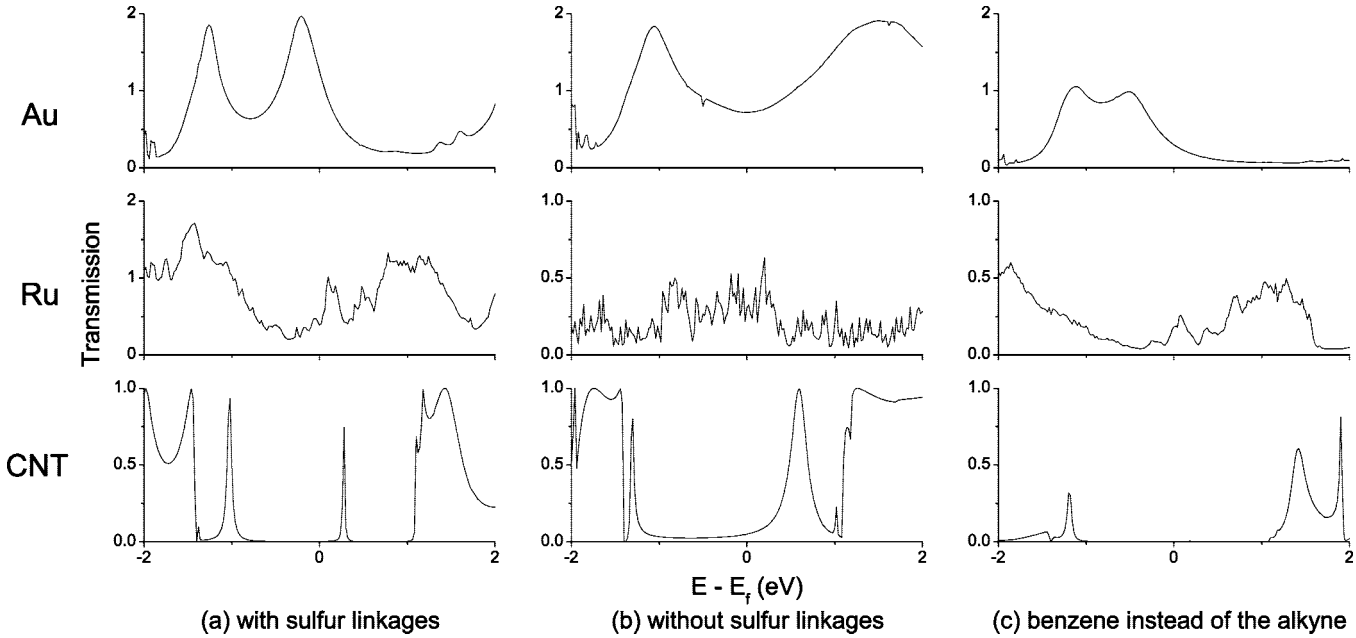

Figure 3. Transmission curves of Au, Ru, and CNT electrodes for an alkyne molecule (a) with the sulfur linkage and (b) without the sulfur linkage. The transmission curves in (c) are calculated after the alkyne molecule is replaced by a benzene molecule.

in systems with Ru or CNT electrodes. The gaps observed in transmission curves are different from those of the isolated molecule due to readjustment of energy levels when electrodes are attached. The broadening tendency of peaks remains more or less the same as before, suggesting that they are strongly influenced by the nature of electrode materials.

We note that some of these characteristics could be traced in the literature. The transmission through the Au electrodes sandwiching a conjugated molecule was reported.[43] The rugged transmission curves were noted in Ru electrode systems.[44,45] These studies showed that transmission curves are quite sensitive to the contact structure. Nevertheless, it can be seen that the characteristics of electrodes that we derived are kept under changes in contact structure. In the case of a CNT, various linking methods were proposed.[46,47] The covalent and one-dimensional nature of the junction bonding in a CNT opens a wealth of possibility in the junction structure. In most cases, the almost zero transmission gap and well-separated peaks with small broadening are observable.

We also note that these characteristics given by electrodes are most evident when it comes to experimentally realized linkage−electrode combinations. As stated earlier, gold electrodes are most widely used with sulfur linkages, Ru with direct covalent bonds to end carbons, and CNT with amide linkages. The Au and Ru cases correspond to Figure 3a and b, respectively. The CNT case is shown in Figure 4 with the optimized geometry. Figure 5 clearly demonstrates how such differences in transmissions are manifested in $I-V$ characteristics. Indeed, the gold electrode shows an almost linear $I-V$ curve, whereas the CNT electrodes lead to nonlinear curves. Note also that Au gives about an order of magnitude larger current than the CNT. It results from large broadening of the transmission curve. The "CNT−amide" case clearly shows the effect of the zero transmission gap. The current is almost zero until 1.5 V, but it surges thereafter. It is the LUMO of the alkyne which contributes to the surge since the peak corresponding to the HOMO is small compared to that of the LUMO. The "CNT−S" case also displays an intriguing behavior. It also surges at around 1.0 V, although it is not as abrupt as the "CNT−amide" case.

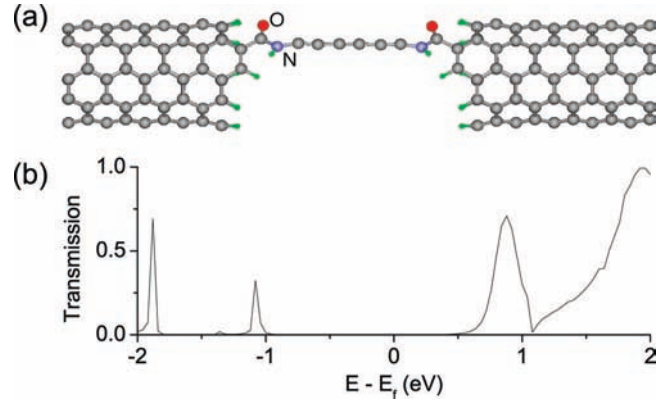

Figure 4. (a) The geometry of the CNT alkyne device where amide linkages are used to connect electrodes and the central molecule. Black lines separate the scattering region at the center from the left and right electrode regions. (b) The transmission curve at a zero bias voltage of the above system.

Its rate of change (dI/dV) varies a lot, whose origin lies in discrete peaks of the transmission, which again originate from discrete molecular levels. In summary, the alkyne molecule is merely a resistor when it is connected to the Au or Ru electrode, whereas it shows the highly nonlinear behavior exhibiting unique characteristics of the molecule when it is attached to the CNT electrode. Thus, the $I-V$ curves of the CNT alkyne system illustrate that the characteristics of a nanodevice can be attributed strongly to the choice of an electrode beside the choice of linkage.

Our study shows that different electrodes give rise to a different broadening extent for the given molecular energy levels and different alignment of the energy levels with respect to the Fermi energy of the electrode. These effects should have implications on determining the function of molecular electronic devices. For example, the CNT electrode would be more suitable to derive nonlinear $I-V$ curves from a particular molecule, compared with Au or Ru electrodes that tend to lead to almost linear $I-V$ characteristics. On the other hand, many experimental observations have shown that electric currents strongly depend on a device molecule even for the same electrode and linkers.

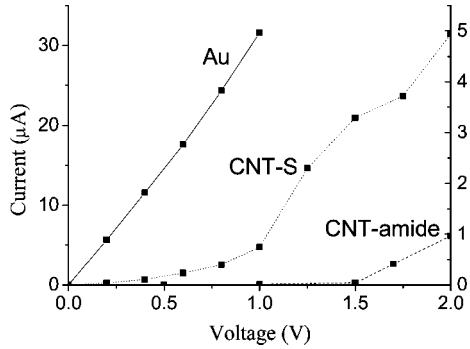

Figure 5. *I*−*V* curves of the alkyne with the gold electrode and two types of CNT electrodes. "CNT−S" and "CNT−amide" denote the cases with the sulfur linkages and the amide linkages, respectively. The scale of the current on the left is for Au, while that on the right is for CNTs.

It is because electrical currents through a molecule are a consequence of complicated interplay between molecular energy level spacing, characteristics of each molecular orbital, their interactions with linkages and electrodes, changes of a molecular structure under bias, and so on. Thus, the electrode effect should be considered not as a determining factor but as a useful factor characterizing molecular transport properties, with the readjustment of each molecular energy level.

IV. Conclusion

The dependence of the transmission function on different types of an electrode material has been examined using the nonequilibrium Green's function method coupled with the density functional theory scheme. The systems investigated are Au, Ru, and CNT electrodes. We observed that the transmission through a molecular device with the Au electrode exhibits conspicuous peaks with large broadening. In the case of the Ru electrode, the contributions from the flat d bands to the incoming states are so strong that little molecular features are reflected on the transmission curve. On the other hand, the CNT electrode shows discrete and sharp peaks in the transmission curve and offers the (almost) zero transmission gap, enabling a device to exhibit nonlinear current−voltage characteristics. In this way, an electrode material in addition to a molecule or linker plays a unique role in determining electron transport properties through the entire device. These features should be considered in designing molecular electronic devices.

Acknowledgment. This work is affectionately dedicated to Professor George C. Schatz, an outstanding scientist on the occasion of his 60th birthday. This work was supported by GRL(KICOS), WCU(KOSEF: R32-2008-000-10180-0), KOSEF (EPB Center: R11-2008-052-01000), BK21, and KISTI (KSC-2008-K08-0002).

References and Notes

(1) Joachim, C.; Gimzewski, J. K.; Aviram, A. *Nature* **2000**, *408*, 541.
(2) Aviram, A.; Ratner, M. A. *Chem. Phys. Lett.* **1974**, *29*, 277.
(3) Reed, M. A.; Zhou, C.; Muller, C. J.; Burgin, T. P.; Tour, J. M. *Science* **1997**, *278*, 252.
(4) Chen, J.; Reed, M. A.; Rawlett, A. M.; Tour, J. M. *Science* **1999**, *286*, 1550.
(5) Nitzan, A.; Ratner, M. A. *Science* **2003**, *300*, 1384.
(6) Nardelli, M. B. *Phys. Rev. B* **1999**, *60*, 7828.
(7) Mujica, V.; Roitberg, A. E.; Ratner, M. *J. Chem. Phys.* **2000**, *112*, 6834.
(8) Brandbyge, M.; Mozos, J. L.; Ordej, P.; Taylor, J.; Stokbro, K. *Phys. Rev. B* **2002**, *65*, 165401.
(9) Rocha, A. R.; Garcia-Suarez, V. M.; Bailey, S. W.; Lambert, C. J.; Ferrer, J.; Sanvito, S. *Nat. Mater.* **2005**, *4*, 335.
(10) Taylor, J.; Guo, H.; Wang, J. *Phys. Rev. B* **2001**, *63*, 245407.
(11) Palacios, J. J.; Perez-Jimenez, A. J.; Louis, E.; SanFabi, E.; Verg, J. A. *Phys. Rev. B* **2002**, *66*, 035322.
(12) Tao, N. J. *Nat. Nanotechnol.* **2006**, *1*, 173.
(13) Bevan, K. H.; Kienle, D.; Guo, H.; Datta, S. *Phys. Rev. B* **2008**, *78*, 035303.
(14) Zhang, W.; Lu, W.; Guo, H.; Wang, E. G. *Phys. Rev. B* **2007**, *75*, 193410.
(15) Waldron, D.; Haney, P.; Larade, B.; MacDonald, A.; Guo, H. *Phys. Rev. Lett.* **2006**, *96*, 166804.
(16) Kim, W. Y.; Kim, K. S. *Nat. Nanotechnol.* **2008**, *3*, 408.
(17) Cheng, D.; Kim, W. Y.; Min, S. K.; Nautiyal, T.; Kim, K. S. *Phys. Rev. Lett.* **2006**, *96*, 096104.
(18) Kim, W. Y.; Choi, Y.; Kim, K. S. *J. Mater. Chem.* **2008**, *18*, 4510.
(19) Ke, S. H.; Baranger, H. U.; Yang, W. *J. Am. Chem. Soc.* **2004**, *126*, 15897.
(20) Xue, Y.; Ratner, M. A. *Phys. Rev. B* **2004**, *69*, 085403.
(21) Lawson, J. W.; Bauschlicher, J. C. W. *Phys. Rev. B* **2006**, *74*, 125401.
(22) Andrews, D. Q.; Cohen, R.; Van Duyne, R. P.; Ratner, M. A. *J. Chem. Phys.* **2006**, *125*, 174718.
(23) Tarakeshwar, P.; Palacios, J. J.; Kim, D. M. *IEEE Trans. Nanotechnol.* **2008**, *7*, 124.
(24) Palacios, J. J.; Tarakeshwar, P.; Kim, D. M. *Phys. Rev. B* **2008**, *77*, 113403.
(25) Ulman, A. *Chem. Rev.* **1996**, *96*, 1533.
(26) Tulevski, G. S.; Myers, M. B.; Hybertsen, M. S.; Steigerwald, M. L.; Nuckolls, C. *Science* **2005**, *309*, 591.
(27) Guo, X.; Small, J. P.; Klare, J. E.; Wang, Y.; Purewal, M. S.; Tam, I. W.; Hong, B. H.; Caldwell, R.; Huang, L.; O'Brien, S. *Science* **2006**, *311*, 356.
(28) Dekker, C. *Phys. Today* **1999**, *52*, 22.
(29) Avouris, P. *Acc. Chem. Res.* **2002**, *35*, 1026.
(30) Kim, W. Y.; Kwon, S. K.; Kim, K. S. *Phys. Rev. B* **2007**, *76*, 33415.
(31) Hong, B.; Lee, J.; Beetz, T.; Zhu, Y.; Kim, P.; Kim, K. *J. Am. Chem. Soc.* **2005**, *127*, 15336.
(32) Hong, B.; Small, J.; Purewal, M.; Mullokandov, A.; Sfeir, M.; Wang, F.; Lee, J.; Heinz, T.; Brus, L.; Kim, P. *Proc. Natl. Acad. Sci. U.S.A.* **2005**, *102*, 14155.
(33) Kim, W. Y.; Kim, K. S. *J. Comput. Chem.* **2008**, *29*, 1073.
(34) Lindsay, S. M.; Ratner, M. A. *Adv. Mater.* **2007**, *19*, 23.
(35) Dadosh, T.; Gordin, Y.; Krahne, R.; Khivrich, I.; Mahalu, D.; Frydman, V.; Sperling, J.; Yacoby, A.; Bar-Joseph, I. *Nature* **2005**, *436*, 677.
(36) Soler, J. M.; Artacho, E.; Gale, J. D.; Garc, A.; Junquera, J.; Ordej, P.; Sanchez-Portal, D. *J. Phys.: Condens. Matter* **2002**, *14*, 2745.
(37) Perdew, J. P.; Burke, K.; Ernzerhof, M. *Phys. Rev. Lett.* **1996**, *77*, 3865.
(38) Sancho, M.; Sancho, J.; Rubio, J. *J. Phys. F: Met. Phys.* **1984**, *14*, 1205.
(39) Ke, S.-H.; Baranger, H. U.; Yang, W. *J. Chem. Phys.* **2007**, *126*, 201102.
(40) Toher, C.; Filippetti, A.; Sanvito, S.; Burke, K. *Phys. Rev. Lett.* **2005**, *95*, 146402.
(41) Heyd, J.; Scuseria, G. E.; Ernzerhof, M. *J. Chem. Phys.* **2003**, *118*, 8207.
(42) Neaton, J. B.; Hybertsen, M. S.; Louie, S. G. *Phys. Rev. Lett.* **2006**, *97*, 216405.
(43) Ke, S.-H.; Baranger, H. U.; Yang, W. *J. Chem. Phys.* **2007**, *127*, 144107.
(44) Hou, S.; Chen, Y.; Shen, X.; Li, R.; Ning, J.; Qian, Z.; Sanvito, S. *Chem. Phys.* **2008**, *354*, 106.
(45) Ning, J.; Qian, Z.; Li, R.; Hou, S.; Rocha, A. R.; Sanvito, S. *J. Chem. Phys.* **2007**, *126*, 174706.
(46) Ke, S.-H.; Baranger, H. U.; Yang, W. *Phys. Rev. Lett.* **2007**, *99*, 146802.
(47) del Valle, M.; Gutierrez, R.; Tejedor, C.; Cuniberti, G. *Nat. Nanotechnol.* **2007**, *2*, 176.

JP810467Q